applied sciences

MDPI

Article

The Effect of Different Optical Clearing Agents on the Attenuation Coefficient and Epidermal Thickness of Human Skin Assessed by Optical Coherence Tomography

Maria Varaka [1], Martha Z. Vardaki [2], Georgios Gaitanis [3], Ioannis D. Bassukas [3] and Nikolaos Kourkoumelis [1,*]

[1] Department of Medical Physics, School of Health Sciences, University of Ioannina, 45110 Ioannina, Greece
[2] Institute of Chemical Biology, National Hellenic Research Foundation, 11635 Athens, Greece
[3] Department of Skin and Venereal Diseases, Faculty of Medicine, School of Health Sciences, University of Ioannina, 45110 Ioannina, Greece
* Correspondence: nkourkou@uoi.gr

Abstract: *Background*: Optical coherence tomography (OCT) is a non-invasive imaging technique based on the interferometry of backscattered light. However, strong light scattering hinders its applicability in clinical dermatology. The strength of scattering is exemplified by the attenuation coefficient which is the rate of OCT signal decay in depth. Attenuation can be reduced by topical application of hyperosmotic liquids with a high refractive index, namely optical clearing agents (OCAs). In this study, we assessed the impact of different OCAs to enhance skin optical permeability in OCT images. In vivo tests were carried out to determine the OCT attenuation coefficient (μ_{OCT}) and epidermal thickness in the treated and untreated epidermis. *Methods*: Four OCAs were studied: Propylenglycol, propylenglycol combined with oleic acid in equal proportions (1:1 v/v), Vaseline, and liquid Vaseline. Percentage change of μ_{OCT} and epidermal thickness were estimated by OCT imaging of a healthy forearm skin, prior to the application of each OCA and after the application, at two time points, t_1 = 5 min, and t_2 = 90 min. μ_{OCT} was quantitatively obtained by fitting the OCT signal to a single scattering model. *Results*: The application of OCAs induced significant changes in both μ_{OCT} (decreased) and epidermal thickness (increased). The synergistic effect of the combined propylenglycol with oleic acid reduced the μ_{OCT} by 43% while propylenglycol induced the highest increase (33%) in epidermal thickness, both at t_2. *Conclusions*: Topical administration of propylenglycol combined with oleic acid can reduce light attenuation in OCT imaging within the clinically relevant timeframe of 90 min.

Keywords: optical coherence tomography; tissue clearing; optical clearing agents; skin

Citation: Varaka, M.; Vardaki, M.Z.; Gaitanis, G.; Bassukas, I.D.; Kourkoumelis, N. The Effect of Different Optical Clearing Agents on the Attenuation Coefficient and Epidermal Thickness of Human Skin Assessed by Optical Coherence Tomography. *Appl. Sci.* **2022**, *12*, 8277. https://doi.org/10.3390/app12168277

Academic Editor: Vladislav Toronov

Received: 26 July 2022
Accepted: 17 August 2022
Published: 19 August 2022

1. Introduction

Optical Coherence Tomography (OCT) is a non-ionizing technique that provides real-time cross-sectional images of living tissues. It is based on low-coherence interferometry with micron-scale spatial resolution and millimeter-scale penetration depth within the optical window of 0.65–1.3 μm [1]. The interferometric measurement of backscattered photons that have preserved their coherence within the imaging volume, enables OCT to record the amplitude and phase of the light signal along with depth information in a 2D image of the scattering medium. Due to the micron resolution and adequate penetration depth, OCT can be employed to display subsurface structural features of tissue sheaths. In clinical settings, OCT finds wide applications in the field of ophthalmology. However, it is still less established as a non-invasive diagnostic method in dermatology where, in contrast to the eye, strong scattering limits the light penetration in the skin. As light absorption is wavelength-dependent, skin imaging is determined by the presence of skin chromophores and OCT devices of 1.3 μm wavelength are typically chosen where absorption remains low [2]. Alterations in tissue morphology trigger changes in the optical properties of the

skin tissue in the near-infrared wavelength range. Hence, the main application of OCT skin imaging is nonmelanoma skin cancers (NMSC) and especially basal cell carcinoma (BCC) due to its distinct spatial localization [3].

Although the interferometric procedure reduces the effect of multiple backscattering, OCT images are inherently noisy and suffer from image artifacts due to intensity and morphological distortions that stem from the different refractive index (RI) of the multiple scatterers lying within coherence distance in the skin tissue [4]. Human tissues have heterogenous composition consisting mainly of interstitial fluid (ISF) and the cytoplasm. The RI of these components, which are largely composed of water, is lower than that of cell scatterers and as result, strong light scattering occurs. This substantial light scattering hinders the effective use of optical technologies in clinical practice despite the superior resolution of techniques that rely on bio-photonics. As a result, it remains a challenging task to overcome scattering effects and attain adequate imaging depth for in vivo studies. To that end, the tissue optical clearing technique can provide reduced scattering in biological tissues utilizing high RI chemical moieties which are termed optical clearing agents (OCA) [5]. Tissue transparency is increased by effectively raising the RI of the ISF to match the RI of the scatterers. For in vivo skin studies, the so-called physical methods are typically preferred given the non-toxicity prerequisite. These are based on a RI matching process to diminish the optical inhomogeneities using an organic and/or aqueous solution [6]. OCAs are selected with a similar to tissue RI and with the ability to diffuse into a tissue specimen substituting water in order to achieve the RI matching. Typically, these agents are in the form of hyperosmotic liquids and cause tissue dehydration and index matching [7,8]. Non-reactive chemical agents, such as sugars (glucose), alcohols (glycerol, diols, etc.) and glycol-based polymers (PEG), have previously demonstrated their ability to reduce OCT optical scattering [7,9–13]. The aim of this study was to assess the impact of four OCAs (Propylenglycol, Propylenglycol combined with Oleic Acid, Vaseline and Liquid Vaseline) on skin optical permeability. The most suitable OCA was determined by the variations of OCT attenuation coefficient (μ_{OCT}) and epidermal thickness which were assessed through OCT image analysis of non-treated skin, measured at two different but clinically relevant time points.

2. Materials and Methods

2.1. Theoretical Model

The attenuation coefficient is the rate of signal decay as light propagates in the tissue. It consists of two components, absorption and scattering, and evolves from local alterations of the tissue's RI which can be directly related to its physiological state and heterogeneity. In the process of absorption, energy conversion takes place while light intensity decreases. Conversely, the elastic scattering in OCT is not an energy conversion event; it involves photon backscattering and elimination of the incident wave. The above processes are characterized by the absorption and scattering coefficients, respectively, which indicate the cross section per path length. The OCT attenuation coefficient (μ_{OCT}) reveals the loss of OCT signal with depth due to the above processes and eventually quantifies the strength of light-tissue interaction in tissues of diverse types or pathologies.

The theoretical description of the OCT signal attenuation is described by models of increasing complexity [14,15]. Still, the most widely used is the single-scattering model which is based on a single exponential decay function according to Beer's law. The model is based on the first-order Born approximation which assumes that the OCT signal is constructed by light that remains coherent after being scattered once. The model provides reliable results for weakly scattering ($\mu_s < 6$ mm^{-1}), and non-absorbing media [16,17] with an accuracy of about 0.8 mm^{-1} for a fixed focus geometry that is typically used in clinical practice [18]. Furthermore, it allows for the spatial determination of the attenuation coefficient of layered samples [19].

The decay of the OCT signal intensity I(z), to a depth z, is given by Equation (1):

$$I(z) \propto e^{-2\mu_{OCT}z} \quad (1)$$

where 2z is the propagation distance in the attenuating tissue which is traversed twice due to the round-trip backscattering event.

By differentiating, Equation (2) is received

$$\mu_{OCT} = -\frac{d\ lnI(z)}{2\ dz} \quad (2)$$

and μ_{OCT} is calculated by fitting the exponential function to the imaging OCT data over a certain depth range [20] as:

$$\mu_{OCT} = -\frac{I(z)}{2\ \Delta \sum_{z+1}^{n} I(z)} \quad (3)$$

where Δ is the registered pixel size and z is the z-th pixel along the depth in the region of interest (ROI) assuming that the attenuation is complete by the nth pixel. Under this approach, the power signal is mapped to a grey-scale value. As the ROI of the OCT tissue image must be selected prior to fitting the exponential curve, we defined the ROI depth limit at the dermo-epidermal junction as this was imposed by the requirement of using at least 15 pixels of the extracted layers for curve fitting [21]. Furthermore, the impact of multiple scattering effects is effectively diminished when only the first 0.19 mm of the OCT signal are considered for fitting [22].

The single scattering OCT model does not account for speckle effects, which typically confound OCT data. Speckle noise is a grainy pattern of bright and dark spots (i.e., signal amplitude fluctuations) on the OCT image due to the multiple ray scattering within tissue coherence distance with random amplitude and phase. The suppression of speckle noise while preserving contrast, is still an active field of research. Typical post-processing software techniques that aim to reduce OCT speckle noise are based on non-local methods. Specifically, the non-local means (NLM) algorithm evaluates the similarity of the intensity and edge information in an image, within areas around the ROI, into weights to perform a weighted maximum likelihood estimation of the noise-free image [23,24]. Here, we employed the NLM denoising algorithm using the optimized opencv python implementation (function: cv.fastNlMeansDenoising() with filterStrength = 10, templateWindowSize = 7, and searchWindowSize = 21) [25,26]. Fiji software was used for image analysis [27].

2.2. Experimental

The OCAs employed in this study were: Propylenglycol (PG), Propylenglycol combined with Oleic Acid in equal proportions (1:1, *v*/*v*) (PGOA), Vaseline (V) and Liquid Vaseline (LV). Vaseline products were purchased by a local drugstore while the other OCAs were purchased in pure form (99%) from Sigma-Aldrich. PG is an aliphatic diol, miscible in water and a common pharmaceutical excipient. It is also used as a cosolvent in formulations to enhance skin permeation due to its mild keratolytic activity. Oleic acid is an unsaturated fatty acid found abundantly in nature and it consists of a hydrophobic tail and a hydrophilic head. Fatty acids are used as intermediates to produce emulsifiers, emollients and lubricants in cosmetic formulations. When OA is applied to the skin, it induces moderate skin irritation and causes local modulation of cytokine production in the viable epidermis [28]. However, it has been widely used to enhance skin penetration in drug delivery and in polymeric micelles for sustained release. It can improve the solubility of lipophilic drugs while it boosts the delivery of both lipophilic and hydrophilic medicaments. The combination of OA with PG yielded an additive effect on the percutaneous absorption of the non-steroidal anti-inflammatory drug Tenoxicam by increasing the flux and decreasing the penetration lag-time [29]. Vaseline consists of a mixture of liquid and solid hydrocarbons with improved spreading and occlusive properties on the skin. Being additionally a cost-effective product, it is frequently used as a vehicle for pharmaceutical

compounds or as a base for various creams and ointments. Liquid Vaseline has a similar composition to Vaseline, and it has a smoother texture as it is combined with minerals and microcrystalline wax.

Each OCA was tested on the right volar forearm of the same healthy volunteer (Caucasian male, 50 years of age, Fitzpatrick skin type III) after informed consent was obtained. The procedure was supervised by expert dermatologists who also performed the OCT measurements via the normal clinical OCT imaging routine. OCT B-scans were recorded from the forearm skin (Figure 1). Additional images were acquired from the same anatomical site, at two time points, to estimate the percentage change in both the attenuation coefficient and epidermal thickness. Specifically, skin imaging took place just after the application of each OCA (t_1 = 5 min) and at t_2 = 90 min afterward.

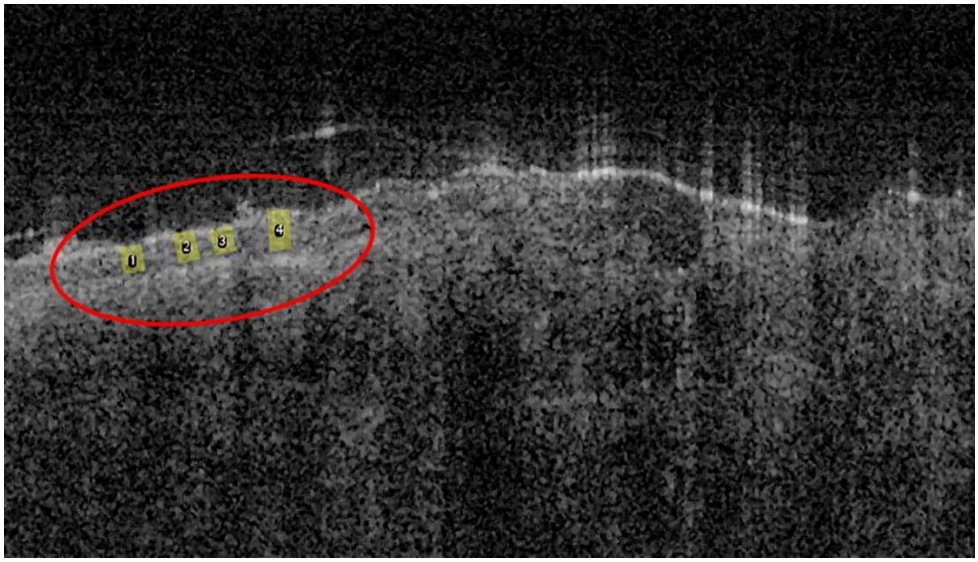

Figure 1. Representative OCT image acquired from the forearm of a healthy volunteer with four ROIs (highlighted with yellow in the red ellipse).

Epidermal thickness was inferred through OCT image analysis, by measuring the distance from the skin surface to the dermo-epidermal junction i.e., in the transition between the signal from the epidermis and the brighter signal from the dermis. Four ROIs in each calibrated OCT image were used and analyzed using Fiji software. It is important to note that the refractive index of the tissue was not taken into account. Thus, the measurements do not correspond to physical, but to optical distances.

OCT measurements were carried out with the OCT NITID system (Dermalumics, Spain), a portable OCT system with a light source at a central wavelength of 1300 nm, axial and lateral resolution at 11 and 12 μm, respectively, and penetration depth of 1.5 mm. OCT 2D scans were greyscale images with height = 512 pixels and width = 1275 pixels. Statistical analysis of μ_{OCT} and epidermal thickness measurements were performed with the Brown–Forsythe equality of means test (α = 0.05), where variances are not assumed to be equal, and normality is not certain, due to the small size of the datasets.

3. Results

Figure 2a depicts the decrease in signal attenuation through tissue after the application of each OCA. The mean value of μ_{OCT} (4.1 mm^{-1}) for the upper dermis of a healthy forearm without prior OCA application is near to that reported in the literature with the OCT technique of 4.2–4.6 mm^{-1} [30,31]. The application of OCAs on the skin induced a decrease of μ_{OCT} in all cases. However, the kinetics of skin scattering alteration varies considerably with the different OCAs. For some OCAs, such as V and LV, the μ_{OCT} decreases almost immediately, and is significantly depressed in five minutes (time point t_1)

after the application and has returned to pretreatment levels 85 min later (time point t_2). On the contrary, the reduction rate of skin scattering is substantially slower with PG and PGOA. A significant μ_{OCT} decrease is found only 90 min after the OCA application. The highest degree of reduction in the μ_{OCT} of healthy human skin with the application of OCAs was found with PGOA application (43%). The mean normalized values of epidermal thickness with and without OCA are depicted in Figure 2b. With all studied OCAs, the epidermal thickness increased monotonically and reached its highest value of ~106 μm at t_2 after applying PG. The mean epidermal thickness was found to be ~79 μm, which resembles the bibliographic value [32].

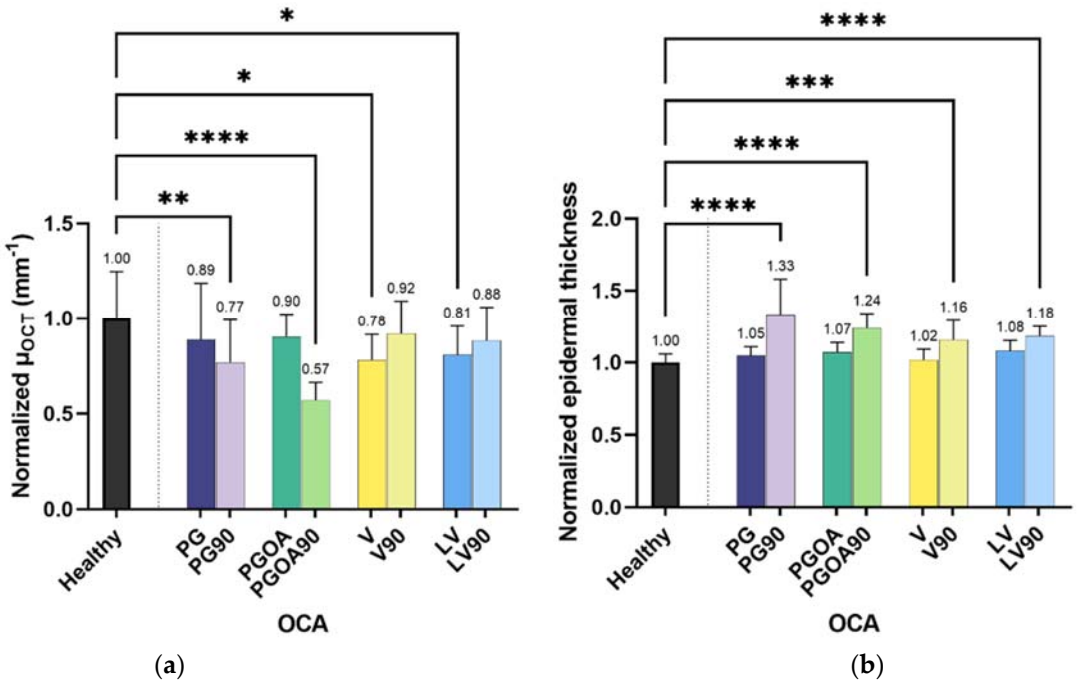

Figure 2. Normalized changes in the signal attenuation coefficient μ_{OCT} (**a**) and in epidermal thickness (**b**) of non-treated skin after the application of four different OCAs at two different times t_1 = 5 min and t_2 = 90 min (x-axis, no name suffix and suffix "90", respectively). The number of asterisks denotes the decreasing *p*-value whereas $p \leq 0.05$, $p \leq 0.01$, $p \leq 0.001$ and $p \leq 0.0001$ are symbolized by 1–4 asterisks. Raw mean values are presented in Tables S1 and S2 (Supplementary Information).

4. Discussion

The uppermost skin layer is the stratum corneum (SC). The role of this skin barrier is to prevent excessive moisture loss and to impede the penetration of potentially unsafe substances into the body. At the same time, the role of SC is crucial for the absorption process of most skin formulations by passive diffusion. SC is composed of approximately 15–25 layers of corneocytes suspended in an extracellular hydrophobic matrix of lipid bilayers [33]. The lipid bilayer space consists of a hydrophilic region in between two hydrophobic ones. Due to its hydrophobic nature, lipid-soluble substances can penetrate SC mainly through the intercellular tissue compartment. To circumvent the limited permeation properties of SC a number of methods have been proposed such as tape-stripping, laser abrasion, electroporation, sonophoresis and iontophoresis [34]. In addition, it has been noted that the SC swells considerably when hydrated and increases its permeability [35]. Penetration enhancers, such as OCAs, can effectively lower the permeation barrier of SC without damaging the viable cells. Due to their hyperosmotic properties when applied on the skin tissue surface, OCAs induce water flux from the interstitial space into the superficial tissue layers, increasing the osmolality of ISF. The process leads to the desired RI matching effect through the swelling of SC and the decrease of μ_{OCT}. In our experiments, all OCAs significantly increase the thickness of the epidermis (Figure 2b). PG induced

the highest increase in epidermal thickness at t_2 (+33%). PG is a hydrophilic molecule and can be attached to the polar head group of the lipid bilayers increasing the interfacial area per lipid without changes in the short or long lamellar spacing of the SC membrane but with some possible alterations of the intracellular α- or β-keratin probably due to the displacement of water [36,37]. This results in the swelling of the intracellular hydrophilic space of the SC and in the increase of epidermal thickness. On the other hand, OA induces SC lipid fluidization and the formation of a new disordered lipid phase [38]. OA consists of a hydrophobic tail and a hydrophilic head. The hydrophobic part lowers the barrier of SC by disrupting the lipid layers, increasing the permeability of the hydrophilic PG [39]. V and LV also increase the water content in SC causing a swelling effect. However, these hydrophobic molecules (OA, V and LV) prevent the high flux of water to the upper SC. In contrast, PG enhances this phenomenon due to its hydrophilic properties, resulting in the observed maximum epidermal thickness. Still, it is known that PG is hygroscopic and adsorbs water until saturation, inhibiting complete dehydration of the tissue [40].

PGOA achieved the lowest μ_{OCT} at t_2 (Figure 2b). Previous studies have shown that when PG and OA are combined, skin permeation is increased as a result of two different synergistic mechanisms: PG solvates the α-keratin of corneocytes while OA acts on the lipid disruption [29,41]. Hence, the presence of OA enhances the multidirectional diffusion of PG into the skin and the OCA uptake saturates in 2–3 h (>t_2). Within the time frame of our experiments, we observed the results of the combined PGOA OCA towards the significant decrease of μ_{OCT} which was the highest among all the tested agents. Significant, albeit lower, reduction was also achieved by PG at t_2. The penetrating activity of PG seems to be crucial for lowering μ_{OCT}. Studies have shown that a large proportion of light scattering from cells happens on the subcellular components and structures at the microscopic scale [42]. Therefore, for RI matching, OCAs must follow a two-stage diffusion scheme, where the initial diffusion into the ISF is followed by diffusion into the intracellular compartments through the cell's membrane. When PG is applied to the skin, it diffuses into the intercellular space causing tissue dehydration. The diffusion rate must be lower than the water flux to the tissue surface due to the high osmolarity of the solution and the molecular size of PG. This is further supported by Figure 2 where PG maximizes the epidermal thickness at t_2 without achieving the lowest μ_{OCT}. The combination of PG and OA in PGOA, increases the diffusion rate of PG which, within the time frame of t_2, subtracts intercellular water out from the tissue and ISF from the cells. The diffusion increases the RI of the sample volume while dehydration enhances the reflectance signal. PG undergoes passive diffusion through cells [43,44] and during the second diffusion stage will eventually achieve a subcellular RI matching. However, due to the molecule's hydrophilicity, tissue re-hydration could happen at this stage with a negative effect on image contrast as it was previously observed for glycerol [7]. Yet, PG and PGOA equilibrium was reported to be achieved in a time scale beyond t_2 (2.5–3.5 h) [41,45,46]. Therefore, we conclude that 90 min is a suitable period for OCT skin measurements as it is tolerable by patients and yields improved biophysical markers in terms of epidermal thickness and μ_{OCT}. An inverted scheme appeared with V and LV resulting in reduced μ_{OCT} mostly at the time of application (t_1). Vaseline is an occlusive emollient that forms a film on the skin surface increasing the skin's moisturizing ability [47]. The elevated water content contributes to the increased epidermal thickness (Figure 2b) while reducing the SC density and consequently the μ_{OCT}. At t_2, V and LV μ_{OCT} values increase due to the fact that these OCAs mostly remain at the SC level with declining concentration over time [47].

5. Conclusions

We have studied the tissue optical clearing effect of four osmotically active agents, PG, PGOA, V and LV using OCT. The application of hyperosmotic agents on skin tissue has been repeatedly shown to reduce random scattering within the OCT imaging volume due to RI matching and tissue dehydration. In this study, PGOA was found to be the most effective agent in lowering the light attenuation through skin tissues over a period

of 90 min. At the same time, PG causes significant tissue dehydration which is depicted in the elevated epidermal thickness. OCT is a morphological imaging technique superior to ultrasound in terms of resolution and ease of handling. Topical administration of PG combined with OA (1:1 v/v) within a clinically relevant timeframe, can enhance tissue differentiation in OCT imaging due to skin dehydration and reduced μ_{OCT}. Still, further work is required to elucidate the contribution of each OCA to skin optical permeability. This will include a population of varying ages, different anatomic regions and multiple solution concentrations.

Supplementary Materials: The following supporting information can be downloaded at: https://www.mdpi.com/article/10.3390/app12168277/s1, Table S1: Mean μ_{OCT} values with standard deviation (SD) estimated by the iterative analysis of four OCT image ROIs at time points t_1 and t_2; Table S2: Mean epidermal thickness values with SD estimated by the iterative analysis of four OCT image ROIs at time points t_1 and t_2.

Author Contributions: Conceptualization, G.G., I.D.B. and N.K.; Data curation, M.V., M.Z.V., G.G. and N.K.; Formal analysis, M.V., M.Z.V. and N.K.; Project administration, N.K.; Supervision, N.K.; Validation, M.V.; Writing—original draft, N.K.; Writing—review & editing, M.Z.V., G.G., I.D.B. and N.K. All authors have read and agreed to the published version of the manuscript.

Funding: This research received no external funding.

Institutional Review Board Statement: University Hospital of Ioannina, 15/19-6-2019(5).

Informed Consent Statement: Informed consent was obtained from all subjects involved in the study.

Data Availability Statement: Data are available on specific request to the corresponding author.

Conflicts of Interest: The authors declare no conflict of interest.

References

1. Olsen, J.; Holmes, J.; Jemec, G.B.E. Advances in optical coherence tomography in dermatology—A review. *J. Biomed. Opt.* **2018**, *23*, 040901. [CrossRef] [PubMed]
2. Israelsen, N.M.; Maria, M.; Mogensen, M.; Bojesen, S.; Jensen, M.; Haedersdal, M.; Podoleanu, A.; Bang, O. The value of ultrahigh resolution OCT in dermatology—Delineating the dermo-epidermal junction, capillaries in the dermal papillae and vellus hairs. *Biomed. Opt. Express* **2018**, *9*, 2240. [CrossRef] [PubMed]
3. Zakharov, V.P.; Bratchenko, I.A.; Artemyev, D.N.; Myakinin, O.O.; Kozlov, S.V.; Moryatov, A.A.; Orlov, A.E. 17—Multimodal Optical Biopsy and Imaging of Skin Cancer. In *Neurophotonics and Biomedical Spectroscopy*; Alfano, R.R., Shi, L., Eds.; Elsevier: Amsterdam, The Netherlands, 2019; pp. 449–476. ISBN 978-0-323-48067-3.
4. Liew, Y.M.; McLaughlin, R.A.; Wood, F.M.; Sampson, D.D. Reduction of image artifacts in three-dimensional optical coherence tomography of skin in vivo. *J. Biomed. Opt.* **2011**, *16*, 116018. [CrossRef] [PubMed]
5. Zhu, D.; Larin, K.V.; Luo, Q.; Tuchin, V.V. Recent progress in tissue optical clearing. *Laser Photonics Rev.* **2013**, *7*, 732–757. [CrossRef]
6. Costantini, I.; Cicchi, R.; Silvestri, L.; Vanzi, F.; Pavone, F.S. In-Vivo and ex-vivo optical clearing methods for biological tissues: Review. *Biomed. Opt. Express* **2019**, *10*, 5251. [CrossRef]
7. He, Y.; Wang, R.K. Dynamic optical clearing effect of tissue impregnated with hyperosmotic agents and studied with optical coherence tomography. *J. Biomed. Opt.* **2004**, *9*, 200. [CrossRef]
8. Vargas, G.; Chan, E.K.; Barton, J.K.; Rylander, H.G., III; Welch, A.J. Use of an agent to reduce scattering in skin. *Lasers Surg. Med.* **1999**, *24*, 133–141. [CrossRef]
9. Zhi, Z.; Han, Z.; Luo, Q.; Zhu, D. Improve optical clearing of skin in vitro with propylene glycol as a penetration enhancer. *J. Innov. Opt. Health Sci.* **2009**, *02*, 269–278. [CrossRef]
10. Larina, I.V.; Carbajal, E.F.; Tuchin, V.V.; Dickinson, M.E.; Larin, K.V. Enhanced OCT imaging of embryonic tissue with optical clearing. *Laser Phys. Lett.* **2008**, *5*, 476–479. [CrossRef]
11. Proskurin, S.G.; Meglinski, I.V. Optical coherence tomography imaging depth enhancement by superficial skin optical clearing. *Laser Phys. Lett.* **2007**, *4*, 824–826. [CrossRef]
12. Wen, X.; Jacques, S.L.; Tuchin, V.V.; Zhu, D. Enhanced optical clearing of skin in vivo and optical coherence tomography in-depth imaging. *J. Biomed. Opt.* **2012**, *17*, 066022. [CrossRef] [PubMed]
13. Khan, M.H.; Choi, B.; Chess, S.; Kelly, K.M.; McCullough, J.; Nelson, J.S. Optical clearing of in vivo human skin: Implications for light-based diagnostic imaging and therapeutics. *Lasers Surg. Med.* **2004**, *34*, 83–85. [CrossRef] [PubMed]
14. Fiske, L.D.; Aalders, M.C.G.; Almasian, M.; van Leeuwen, T.G.; Katsaggelos, A.K.; Cossairt, O.; Faber, D.J. Bayesian analysis of depth resolved OCT attenuation coefficients. *Sci. Rep.* **2021**, *11*, 2263. [CrossRef] [PubMed]

15. Gong, P.; Almasian, M.; van Soest, G.; de Bruin, D.M.; van Leeuwen, T.G.; Sampson, D.D.; Faber, D.J. Parametric imaging of attenuation by optical coherence tomography: Review of models, methods, and clinical translation. *J. Biomed. Opt.* **2020**, *25*, 040901. [CrossRef] [PubMed]
16. Yang, Y.; Wang, T.; Biswal, N.C.; Wang, X.; Sanders, M.; Brewer, M.; Zhu, Q. Optical scattering coefficient estimated by optical coherence tomography correlates with collagen content in ovarian tissue. *J. Biomed. Opt.* **2011**, *16*, 090504. [CrossRef] [PubMed]
17. Lee, P.; Gao, W.; Zhang, X. Performance of single-scattering model versus multiple-scattering model in the determination of optical properties of biological tissue with optical coherence tomography. *Appl. Opt.* **2010**, *49*, 3538. [CrossRef] [PubMed]
18. Faber, D.J.; van der Meer, F.J.; Aalders, M.C.G.; van Leeuwen, T.G. Quantitative measurement of attenuation coefficients of weakly scattering media using optical coherence tomography. *Opt. Express* **2004**, *12*, 4353. [CrossRef] [PubMed]
19. van der Meer, F.J.; Faber, D.J.; Sassoon, D.M.B.; Aalders, M.C.; Pasterkamp, G.; van Leeuwen, T.G. Localized measurement of optical attenuation coefficients of atherosclerotic plaque constituents by quantitative optical coherence tomography. *IEEE Trans. Med. Imaging* **2005**, *24*, 1369–1376. [CrossRef] [PubMed]
20. Vermeer, K.A.; Mo, J.; Weda, J.J.A.; Lemij, H.G.; de Boer, J.F. Depth-Resolved model-based reconstruction of attenuation coefficients in optical coherence tomography. *Biomed. Opt. Express* **2014**, *5*, 322. [CrossRef]
21. Chang, S.; Bowden, A.K. Review of methods and applications of attenuation coefficient measurements with optical coherence tomography. *J. Biomed. Opt.* **2019**, *24*, 090901. [CrossRef]
22. Kodach, V.M.; Kalkman, J.; Faber, D.J.; van Leeuwen, T.G. Quantitative comparison of the OCT imaging depth at 1300 Nm and 1600 Nm. *Biomed. Opt. Express* **2010**, *1*, 176. [CrossRef] [PubMed]
23. Cuartas-Vélez, C.; Restrepo, R.; Bouma, B.E.; Uribe-Patarroyo, N. Volumetric non-local-means based speckle reduction for optical coherence tomography. *Biomed. Opt. Express* **2018**, *9*, 3354. [CrossRef]
24. Yu, H.; Gao, J.; Li, A. Probability-Based non-local means filter for speckle noise suppression in optical coherence tomography images. *Opt. Lett.* **2016**, *41*, 994–997. [CrossRef] [PubMed]
25. Buades, A.; Coll, B.; Morel, J.-M. Non-Local means denoising. *Image Process. Line* **2011**, *1*, 208–212. [CrossRef]
26. Bradski, G. The openCV library. *Dr. Dobb's J. Softw. Tools* **2000**, *25*, 120–123.
27. Schindelin, J.; Arganda-Carreras, I.; Frise, E.; Kaynig, V.; Longair, M.; Pietzsch, T.; Preibisch, S.; Rueden, C.; Saalfeld, S.; Schmid, B.; et al. Fiji: An open-source platform for biological-image analysis. *Nat. Methods* **2012**, *9*, 676–682. [CrossRef]
28. Boelsma, E.; Tanojo, H.; Boddé, H.E.; Ponec, M. Assessment of the potential irritancy of oleic acid on human skin: Evaluation in vitro and in vivo. *Toxicol. Vitr.* **1996**, *10*, 729–742. [CrossRef]
29. Larrucea, E. Combined effect of oleic acid and propylene glycol on the percutaneous penetration of tenoxicam and its retention in the skin. *Eur. J. Pharm. Biopharm.* **2001**, *52*, 113–119. [CrossRef]
30. Welzel, J.; Bruhns, M.; Wolff, H.H. Optical coherence tomography in contact dermatitis and psoriasis. *Arch. Dermatol. Res.* **2003**, *295*, 50–55. [CrossRef]
31. Schmitt, J.M.; Knüttel, A.; Bonner, R.F. Measurement of optical properties of biological tissues by low-coherence reflectometry. *Appl. Opt.* **1993**, *32*, 6032–6042. [CrossRef]
32. Lintzeri, D.A.; Karimian, N.; Blume-Peytavi, U.; Kottner, J. Epidermal thickness in healthy humans: A systematic review and meta-analysis. *J. Eur. Acad. Dermatol. Venereol.* **2022**, *36*, 1191–1200. [CrossRef] [PubMed]
33. Vávrová, K.; Kováčik, A.; Opálka, L. Ceramides in the skin barrier. *Eur. Pharm. J.* **2017**, *64*, 28–35. [CrossRef]
34. Gorzelanny, C.; Mess, C.; Schneider, S.W.; Huck, V.; Brandner, J.M. Skin barriers in dermal drug delivery: Which barriers have to be overcome and how can we measure them? *Pharmaceutics* **2020**, *12*, 684. [CrossRef] [PubMed]
35. Ruela, A.L.M.; Perissinato, A.; Lino, M.E.D.S.; Mudrik, P.S.; Pereira, G.R. Evaluation of skin absorption of drugs from topical and transdermal formulations. *Braz. J. Pharm. Sci.* **2016**, *52*, 527–544. [CrossRef]
36. Bouwstra, J.A.; de Vries, M.A.; Gooris, G.S.; Bras, W.; Brussee, J.; Ponec, M. Thermodynamic and structural aspects of the skin barrier. *J. Control. Release* **1991**, *15*, 209–219. [CrossRef]
37. Moghadam, S.H.; Saliaj, E.; Wettig, S.D.; Dong, C.; Ivanova, M.V.; Huzil, J.T.; Foldvari, M. Effect of chemical permeation enhancers on stratum corneum barrier lipid organizational structure and interferon alpha permeability. *Mol. Pharm.* **2013**, *10*, 2248–2260. [CrossRef]
38. Boncheva, M.; Damien, F.; Normand, V. Molecular organization of the lipid matrix in intact stratum corneum using ATR-FTIR spectroscopy. *Biochim. Biophys. Acta (BBA)-Biomembr.* **2008**, *1778*, 1344–1355. [CrossRef]
39. Jiang, J.; Zhang, L.; Sergey, G.; Proskurin, S.G.; Wang, R.K. *OCT Image Contrast Improvement of Skin Tissue by Using Oleic Acid as an Enhancer*; SPIE: Bellingham, WA, USA, 2005; Volume 5630, pp. 278–285.
40. Genina, E.A.; Bashkatov, A.N.; Sinichkin, Y.P.; Yanina, I.Y.; Tuchin, V.V. Optical clearing of biological tissues: Prospects of application in medical diagnostics and phototherapy. *JBPE* **2015**, *1*, 22–58. [CrossRef]
41. Atef, E.; Altuwaijri, N. Using Raman spectroscopy in studying the effect of propylene glycol, oleic acid, and their combination on the rat skin. *AAPS PharmSciTech* **2018**, *19*, 114–122. [CrossRef]
42. Mourant, J.R.; Freyer, J.P.; Hielscher, A.H.; Eick, A.A.; Shen, D.; Johnson, T.M. Mechanisms of light scattering from biological cells relevant to noninvasive optical-tissue diagnostics. *Appl. Opt.* **1998**, *37*, 3586. [CrossRef]
43. Edashige, K. Permeability of the plasma membrane to water and cryoprotectants in mammalian oocytes and embryos: Its relevance to vitrification. *Reprod. Med. Biol.* **2017**, *16*, 36–39. [CrossRef]

44. Shu, Z.; Hughes, S.M.; Fang, C.; Huang, J.; Fu, B.; Zhao, G.; Fialkow, M.; Lentz, G.; Hladik, F.; Gao, D. A study of the osmotic characteristics, water permeability, and cryoprotectant permeability of human vaginal immune cells. *Cryobiology* **2016**, *72*, 93–99. [CrossRef] [PubMed]
45. Guo, X.; Guo, Z.Y.; Wei, H.J.; Yang, H.Q.; He, Y.H.; Xie, S.S.; Wu, G.Y.; Zhong, H.Q.; Li, L.Q.; Zhao, Q.L. In vivo quantification of propylene glycol, glucose and glycerol diffusion in human skin with optical coherence tomography. *Laser Phys.* **2010**, *20*, 1849–1855. [CrossRef]
46. Trottet, L.; Merly, C.; Mirza, M.; Hadgraft, J.; Davis, A.F. Effect of finite doses of propylene glycol on enhancement of in vitro percutaneous permeation of loperamide hydrochloride. *Int. J. Pharm.* **2004**, *274*, 213–219. [CrossRef] [PubMed]
47. Meng, H.; Yin, Y.; Wu, W.; Liu, Y.; Li, L.; Dong, Y.; Fan, Y.; Li, Y.; He, Y. Raman spectroscopic analysis of skin penetration and moisturizing effects of bionics vernix caseosa cream compared with Vaseline. *THC* **2021**, *29*, 327–334. [CrossRef] [PubMed]